

Intramolecular charge transfer in π -conjugated oligomers: a theoretical study on the effect of temperature and oxidation state

Massimiliano Aschi · Maira D'Alessandro ·
Monica Pellegrino · Alfredo Di Nola ·
Marco D'Abramo · Andrea Amadei

Received: 15 October 2007 / Accepted: 20 December 2007 / Published online: 11 January 2008
© Springer-Verlag 2008

Abstract Intramolecular charge transfer (ICT) of gaseous π -conjugated oligo-phenyleneethynyls (OPE) induced by a homogeneous applied electric field has been theoretically investigated using a combined approach integrating molecular dynamics (MD) simulations and Perturbed Matrix Method calculations. In line with recent investigations, our results indicate the peculiar role of conformational transitions on OPE electronic properties which reflects on a strong temperature effect on ICT. Electron transfer reactions inducing chemical alteration on OPE, also taken into account in this study, revealed extremely important for explaining non-linear ICT effects and probably plays a central role in the mechanisms underlying molecular transport junctions. Our study further points out the necessity of using MD-based

approach for modelling molecular electronics, even when relatively rigid molecular systems are concerned.

Keywords Molecular electronics · Intramolecular charge transfer · Molecular dynamics · Quantum chemistry

1 Introduction

Molecular electronics (ME) is a new and exciting research area of huge potential technological impact, whose main aim is the design, synthesis and application of molecule-based devices to be used at nanoscopic regime [1–3].

The most fundamental devices for ME are the molecular transport junctions (MTJ) essentially based on one [4] or more molecules physically or chemically encapsulated between two electrodes [5]. The basic features of such junctions rely on the possibility of combining electrode continuum levels with single molecule electronic properties and single molecule orientation [6] offering, at least in principle, a very large variety of technological possible applications. In this respect, the design of MTJ, starting not only from the chemical intuition but also from a reliable theoretical modelling at atomic-molecular level, would provide an important intellectual and technological improvement. Of course any realistic description of the overall MTJ is still theoretically and computationally very demanding. At the same time, it is common opinion that to understand and predict the properties of MTJ it would be important to understand single-molecule physico-chemical features. For this reason, many investigators in the past few years have proposed, and successfully applied, several approaches providing a powerful tool for theoretically addressing single-molecule conductance properties [7–12].

M. Aschi (✉)
Dipartimento di Chimica, Ingegneria Chimica e Materiali
Universita' di L'Aquila, Via Vetoio (Coppito),
67010 L'Aquila, Italia
e-mail: aschi@caspur.it

M. D'Alessandro · A. D. Nola · M. D'Abramo
Dipartimento di Chimica, Universita' di Roma 'La Sapienza',
P.le A. Moro 5, 00185 Roma, Italia

M. Pellegrino
Dipartimento di Ingegneria Elettronica, Universita' di Roma
'La Sapienza', Via Eudossiana 18, 00184 Roma, Italia

M. D'Abramo
Barcelona Supercomputing Center, Torre Girona, c/ Jordi Girona,
31, 08034 Barcelona, Spain

A. Amadei (✉)
Dipartimento di Scienze e Tecnologie Chimiche,
Universita' di Roma 'Tor Vergata', Via della Ricerca Scientifica 1,
00133 Roma, Italy
e-mail: andrea.amadei@uniroma2.it

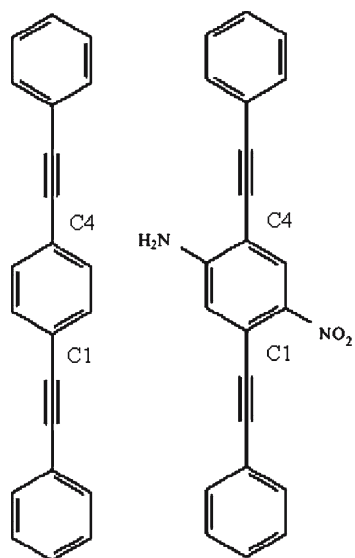


Fig. 1 Schematic view of OPE1 (*left*) and OPE2 molecules

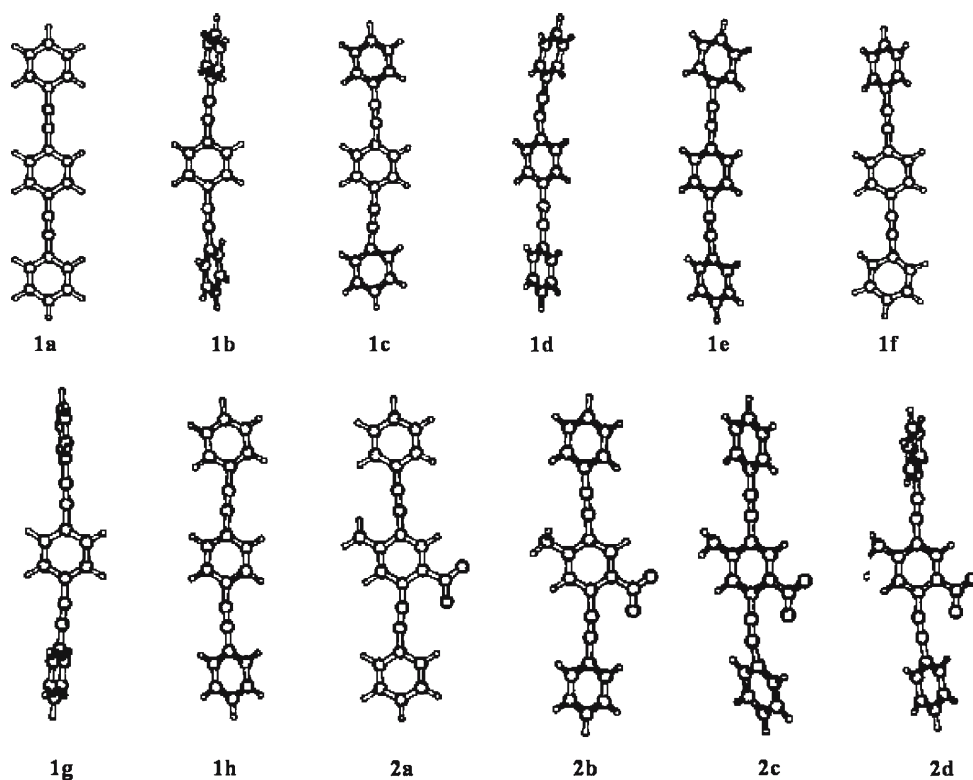
In the very early applications of the above methodologies, essentially all based on the application of the Green's function, molecular geometries were kept frozen or allowed to undergo conformational transitions along pre-defined internal coordinates.

In the past few years, also stimulated by important experimental evidences [13], new computational studies, based on the same approach, have been insisting on the neces-

sity of including conformational transitions on the determination of single-molecule conductance [14]. In this context we have recently shown [15], by using molecular dynamics (MD) simulations and Perturbed Matrix Method (PMM) calculations [16], that even slight thermal fluctuations may produce, in the presence of a suitable electric field, dramatic effects on the intramolecular charge transfer (ICT) of gaseous π -conjugated oligo-phenyleneethynylenes (OPE1 and OPE2) schematically represented in Fig. 1.

More specifically, OPE2 turned out to typically provide a linear response to the applied electric field, in line with previous studies indicating non-linear field response only in the presence of a chemical modification, i.e. reduction [17]. On the other hand, in the case of OPE1, ICT resulted largely affected by conformational equilibria determined by the proper statistical mechanical ensemble of the system. Interestingly, and in a somewhat counter-intuitive fashion, for such a molecule non-linear ICT field response is observed when non-planar, i.e. non-strictly conjugated species (see structures **1b** and **1g** in Fig. 2) are populated at 300 K in the presence of high field [18]. Beyond the above results, our preliminary study has clearly indicated, in line with other investigators [14], that ICT (somewhat related to the actual conductance) should be treated as an *observable* of the system in strict *statistical-mechanical* terms. In this respect whatever modification induced by the action of the environment able in principle to strongly modify the ensemble, e.g. by temperature variations [13] and/or by the change in the oxidation state

Fig. 2 Representative structures of OPE1 (**1a–1h**) and OPE2 (**2a–2d**) free energy basins sampled at the highest temperature



[19,20], should definitely influence the electrical properties of the molecular devices.

In this paper, in which our preliminary results have been completed and extended, we wish to reinforce such a view of ICT by evaluating electric field response of gaseous OPE1 and OPE2, when the system undergoes changes in the temperature or/and oxidation state. Our aim is not to provide an alternative computational approach to describe electronic conductance, but rather to further point out the importance of including thermal fluctuations and chemical alterations in single-molecule conductance modelling.

2 Theoretical and computational section

Molecular dynamics simulations were performed for isolated and uncharged OPE1 and OPE2 without applying any external field. The trajectories were propagated for 12.0 ns and the first 2.0 ns were disregarded from the analysis. The simulations were carried out at 10, 50, 100, 150, 300 and 500 K for both systems using the isokinetic temperature coupling [21], constraining the roto-translational motions [22] to be coherent with the experimental conditions in which the molecule global motions are constrained by the electrodes.

All the bond lengths were constrained using the LINCS algorithm [23]. Note that we used the same force field parameters as described in the earlier article [15]. GROMACS software package [24] was adopted for all the simulations. All the trajectories, carried out at different temperatures, were analysed using essential dynamics (ED) [25].

Briefly, by diagonalizing OPE1 and OPE2 all the atoms positional fluctuation covariance matrix, as provided by the MD simulation, we obtain a set of eigenvectors and eigenvalues. The eigenvectors represent the directions in configurational space and the eigenvalues indicate the mean square fluctuations along these axes. Sorting the eigenvectors by the size of the corresponding eigenvalues, the configurational space can be divided into a low-dimensional (essential) subspace in which most of the positional fluctuations are confined and a high-dimensional subspace in which merely small vibrations occur. In particular, we characterized the thermodynamics as a function of the position in the essential plane spanned by the first and second eigenvectors. The free energy change for any transition from a reference state (ref) to a generic i th state can be calculated from the probabilities P (obtained by the MD simulation) of finding the system in both states i and ref

$$\Delta A_{\text{ref} \rightarrow i} = -RT \ln \frac{P_i}{P_{\text{ref}}} \quad (1)$$

where R is the ideal gas constant and T the (absolute) temperature. We used a 20×20 grid for defining the conformational states in the essential plane. In this way, we obtained a set of

free energy minima describing all the relevant OPE conformational transitions at the different temperatures. For each minimum, we then defined a corresponding free energy basin given by its surrounding region within a free energy variation of 9.0 kJ/mol.

We wish to remark that the available experimental data are usually obtained with OPE chemically adsorbed on the electrodes in such a way their molecular roto-translational motions are essentially constrained and, hence, the external field applied has a fixed orientation in the molecular frame (basically parallel to the average OPE principal axis). In order to provide some sort of relationship between our theoretical-computational results and the information obtained from such an experimental setup, we considered a statistical mechanical ensemble where each OPE molecule, with constrained roto-translational degrees of freedom, may only interact with an electric field parallel to the $C1 \rightarrow C4$ unit vector (see Fig. 1) which corresponds to a completely fixed direction in OPE molecular frame. Moreover, given the weak to moderate field intensity used to reproduce the experimental conditions, we assumed that the free energy basins provided by the MD simulations (not involving the external electric field) still represent all the relevant conformational regions in the presence of the perturbing field.

Therefore, for each free energy minimum we extracted a corresponding relaxed molecular structure which was used to provide the basin electronic properties variation due to the field, i.e. we assume the electronic properties of such relaxed structure as representative of the whole basin.

In correspondence of each of the above structure, representing the l th basin, we described neutral (n) OPE (both OPE1 and OPE2) unperturbed-state by evaluating 11 unperturbed states $|\Phi_{i,nl}^0\rangle$ (i from 1 to 11 for l th basin) using time-dependent density functional theory (TD-DFT) with PBE0 functional [26] in conjunction with $6-31+G(d)$ atomic basis set.¹ The same calculations, repeated also for reduced (r) OPE provided 11 unperturbed states $|\Phi_{i,rl}^0\rangle$. The use of TD-DFT was forced by previous unsuccessful attempts of obtaining such a large set of unperturbed eigenstates by adopting post Hartree-Fock methodologies such as complete active space self-consistent field and configuration interaction. As the conformational analysis was based on the same ensemble obtained by neutral OPE MD simulations, such calculations were carried out on the same structures in anionic state. Such a procedure is motivated by the reasonable assumption that, for each temperature considered, the accessible conformational space of the neutral and reduced OPE molecule is essentially the same. In order to avoid spurious geometrical effects on the quality of the wave

¹ The choice of this level of theory is explained in [15] and references therein included.

function, we carried out a few steps of preliminary energy relaxations. In particular, we first relaxed carbon–hydrogen bonds keeping frozen the MD-extracted geometry. Subsequently, a slight relaxation of the overall framework was carried out by keeping the molecule within the corresponding free-energy basin. Such a local optimization should not significantly modify the basin representative structure, i.e. basin free energy minimum structure, and hence guarantees a proper PMM application. Quantum-chemical calculations were performed using Gaussian 03 package [27].

The above unperturbed states were then used, for each basin, to construct the perturbed Hamiltonian matrix, to be used in the PMM calculations, by applying an external homogeneous electric field (\mathbf{E}) along C1–C4 unit vector \mathbf{b} (See Fig. 1).

Perturbed eigenvectors (\mathbf{c}) from diagonalisation of electronic Hamiltonian in the presence of electric field \mathbf{E} , allowed us to calculate perturbed ground state dipole moment of neutral $\mu_{\text{ni}}(\mathbf{E})$ and reduced $\mu_{\text{ri}}(\mathbf{E})$ molecule for each i th basin. These calculations, as usual, were carried out by evaluating ground state, i.e. state l perturbing electric dipole, using Eq. (2) for the generic k component

$$\mu_{k,\text{ni}} = \mathbf{c}^* \mathbf{T} \left\langle \Phi_{1,\text{ni}}^0 | \hat{\mu}_k | \Phi_{1,\text{ni}}^0 \right\rangle \mathbf{c} \quad (k = x, y \text{ and } z) \quad (2)$$

Using the unperturbed dipole moment for the neutral ($\mu_{\text{ni}}(0)$) and reduced ($\mu_{\text{ri}}(0)$) OPE and defining

$$\begin{aligned} \Delta \mu_{\text{ni}} &= \mu_{\text{ni}}(\mathbf{E}) - \mu_{\text{ni}}(0) \\ \Delta \mu_{\text{ri}} &= \mu_{\text{ri}}(\mathbf{E}) - \mu_{\text{ri}}(0) \end{aligned} \quad (3)$$

we calculated for each i th basin the corresponding intramolecular charge variation for the neutral and reduced OPE by the relations

$$\begin{aligned} \Delta q_{\text{ni}} &= \frac{\Delta \mu_{\text{ni}} \cdot \mathbf{b}}{L} \\ \Delta q_{\text{ri}} &= \frac{\Delta \mu_{\text{ri}} \cdot \mathbf{b}}{L} \end{aligned} \quad (4)$$

with L being the molecular length (about 1.9 nm).

From the perturbed and unperturbed eigenvalues, $U_{\text{ni}}(\mathbf{E})$ and $U_{\text{ni}}(0)$, we can calculate ICT expectation value for the neutral OPE, i.e. $\langle \Delta q \rangle_n$ by using the equation

$$\langle \Delta q \rangle_n = \sum_i P_{\text{ni}}(\mathbf{E}) \Delta q_{\text{ni}} \quad (5)$$

where the equilibrium probability of the i th basin in the presence of the applied field $P_{\text{ni}}(\mathbf{E})$ is expressed by the corresponding unperturbed probability $P_{\text{ni}}(0)$ via

$$P_{\text{ni}}(\mathbf{E}) = \frac{P_{\text{ni}}(0) e^{-\beta \Delta U_{\text{ni}}(\mathbf{E})}}{\sum_l P_{\text{ni}}(0) e^{-\beta \Delta U_{\text{ni}}(\mathbf{E})}} \quad (6)$$

and

$$\Delta U_{\text{ni}}(\mathbf{E}) = U_{\text{ni}}(\mathbf{E}) - U_{\text{ni}}(0) \quad (7)$$

Within the same approximations used in the previous equations, from the perturbed electronic Hamiltonian eigenvalues for OPE⁻, $U_{\text{ri}}(\mathbf{E})$, we can define for each i th basin the Helmholtz free energy change due to the reduction process as

$$\Delta A_i(\mathbf{E}) = A_{\text{ri}}(\mathbf{E}) - A_{\text{ni}}(\mathbf{E}) = U_{\text{ri}}(\mathbf{E}) - U_{\text{ni}}(\mathbf{E}) \quad (8)$$

Therefore, using

$$A_{\text{ri}}(\mathbf{E}) = A_{\text{ni}}(\mathbf{E}) + U_{\text{ri}}(\mathbf{E}) - U_{\text{ni}}(\mathbf{E}) = A_{\text{ni}}(\mathbf{E}) + \Delta A_i(\mathbf{E}) \quad (9)$$

we can calculate the (vertical) free energy, ΔA associated to the reaction



in the presence of the applied field \mathbf{E}

$$\begin{aligned} \Delta A &= -kT \ln \frac{\sum_i e^{-\beta A_{\text{ri}}(\mathbf{E})}}{\sum_i e^{-\beta A_{\text{ni}}(\mathbf{E})}} \\ &= -kT \ln \frac{\sum_i e^{-\beta A_{\text{ni}}(\mathbf{E})} e^{-\beta \Delta A_i(\mathbf{E})}}{\sum_i e^{-\beta A_{\text{ni}}(\mathbf{E})}} \\ &= -kT \ln \sum_i P_{\text{ni}}(\mathbf{E}) e^{-\beta \Delta A_i(\mathbf{E})} \end{aligned} \quad (11)$$

Finally, the expectation value for the ICT in the reduced OPE, i.e. $\langle \Delta q \rangle_r$, can be calculated as

$$\begin{aligned} \langle \Delta q \rangle_r &= \frac{\sum_i e^{-\beta A_{\text{ri}}(\mathbf{E})} \Delta q_{\text{ri}}}{\sum_i e^{-\beta A_{\text{ri}}(\mathbf{E})}} \\ &= \frac{\sum_i e^{-\beta A_{\text{ni}}(\mathbf{E})} e^{-\beta \Delta A_i(\mathbf{E})} \Delta q_{\text{ri}}}{\sum_i e^{-\beta A_{\text{ni}}(\mathbf{E})} e^{-\beta \Delta A_i(\mathbf{E})}} \\ &= \frac{\sum_i P_{\text{ni}}(\mathbf{E}) e^{-\beta \Delta A_i(\mathbf{E})} \Delta q_{\text{ri}}}{\sum_i P_{\text{ni}}(\mathbf{E}) e^{-\beta \Delta A_i(\mathbf{E})}} \end{aligned} \quad (12)$$

3 Results and discussions

3.1 Thermal effects on ICT for OPE1 and OPE2

In Tables 1 and 2 we report the relative stabilities of the free energy basins as emerged by MD simulations at the investigated temperatures for OPE1 and OPE2, respectively.

The representative structures are depicted in Fig. 2 and the related essential geometrical parameters are reported in Tables 3 and 4.

Results show that configurations sampled at 300 K, already described in our preliminary study [15] basically provide the overall conformational repertoire up to 500 K. Both for OPE1 and OPE2 a strong configurational confinement within the fully-planar states (**1c** and **2a**) is observed at least below 100 K. For temperatures higher than 100 K a wider population emerges with the planar species, however, always representing the most stable states.

Table 1 Free energy differences (kJ/mol) calculated at each temperature using Eq. (1) for OPE1 basins from MD simulations and ED analysis (with no field applied)

Species	10 K	50 K	100 K	150 K	200 K	300 K	500 K
1a	–	–	10	6	6	6	6
1b	–	–	6	5	5	5	2
1c	0	0	0	0	0	0	0
1d	–	–	6	6	6	6	9
1e	–	–	6	3	0	0	0
1f	–	–	5	4	0	0	0
1g	–	–	5	5	5	5	2
1h	–	–	4	1	0	0	0

The symbol (–) means that the corresponding basin was never sampled during MD simulation. All the data are affected by an error of ± 2 kJ/mol

Table 2 Free energy differences (kJ/mol) calculated at each temperature using Eq. (1) OPE2 basins from MD simulations and ED analysis (with no field applied)

Species	10 K	50 K	100 K	150 K	200 K	300 K	500 K
2a	0	0	0	0	0	0	0
2b	–	–	6	4	3	3	3
2c	–	–	–	8	3	3	3
2d	–	–	–	8	4	2	2

The symbol (–) means that the corresponding basin was never sampled during MD simulation. All the data are affected by an error of ± 2 kJ/mol

Table 3 Geometrical parameters of the eight basins of OPE1

Basin	φ_1 (°)	φ_2 (°)	τ (°)
1a	0	0	180
1b	–79	–60	175
1c	–20	20	176
1d	24	–20	164
1e	–8	0	172
1f	–40	20	179
1g	–80	–81	175
1h	–19	1	175

φ_1 and φ_2 represent the rotation angles of the upper ring, lower ring with respect the central one, and τ the angle between the geometrical center of the three rings

Table 4 Geometrical parameters of the four basins of OPE2

Basin	φ_1 (°)	φ_2 (°)	τ (°)
2a	0.0	0.0	180
2b	–25	–20	175
2c	12	18	172
2d	–76	100	176

φ_1 and φ_2 represent the rotation angles of the upper ring, lower ring with respect the central one, and τ the angle between the geometrical center of the three rings

We wish to point out, in this respect, that our simulations were carried out by using a barrier height of 4.0 kJ/mol in line with previous computational studies [8]. Recent experimental estimations of such a barrier indicate a value of about 3 kJ/mol [28]. Hence, our simulations may be slightly affected by a systematic error which, however, should not dramatically alter the overall picture.

The use of PMM combined with the above MD/ED results provides, following the equations of the Theory section, the picture diagrammatically shown in Fig. 3 where OPE1 ICT is plotted onto the plane defined by the temperature and the intensity of the applied electric field (voltage).²

The sharp temperature effect on OPE1 ICT may be related, although not directly, to experimental evidences [13]. Moreover, we may define, on the above diagrams of Fig. 3, critical values of temperature and applied field above which non-linear field response may be observed for OPE1.

As a matter of fact at whatever temperature above 100 K it becomes possible to modulate and control non-linear field responses just modulating the applied voltage as depicted in the right-down-side of Fig. 3. At the same time, at voltages higher than 10 V, and lower than –10.0 V, different field–response behaviours can be obtained just changing the temperature (see right-up-side of Fig. 3). In order to provide some relationship between molecular conformations and ICT behaviour, following our preliminary findings [15], we compared OPE1 ICT with the cumulative probability of the rotated species **1b** and **1g**. The result, reported in Fig. 4 clearly confirm the strong relationship between thermodynamic stability of **1b** and **1g** and observed ICT.

Hence, sudden ICT variations observed in our numerical experiments are due to the presence of non fully-conjugated species.

Differently from OPE1, OPE2 did not show any deviation from linearity, at least in the temperature and voltage ranges investigated. However, alteration in the oxidation state may plausibly provide some effect as described in the literature [19,20] and illustrated in the next subsection.

3.2 Effects of chemical modifications at 300 K

As already mentioned in the introduction, recent studies have inferred that the application of the electric field may alter the

² As already reported in our preliminary study [15], the voltage is calculated considering a homogeneous electric field, parallel to the OPE longitudinal axis, and a length (2.0 nm) slightly overestimating the actual OPE length (1.9 nm). For this reason applied voltage cannot be exactly compared to the nominal voltages used in the experimental setups. Nevertheless we wish to stress the fact that electric fields used in the present paper are of the same order of magnitude (sometimes equal to) of the ones used in all the recent investigations (see, for example [11]).

Fig. 3 Left side OPE1 ICT, $\langle \Delta q \rangle_n$ (a.u.), reported on the plane of temperature (RT , kJ/mol) and applied voltage (in volt/10). Right side: isothermal section (300 K) of OPE1 ICT, $\langle \Delta q \rangle_n$, (lower panel) and iso-voltage section (+12V) of OPE1 ICT (upper panel)

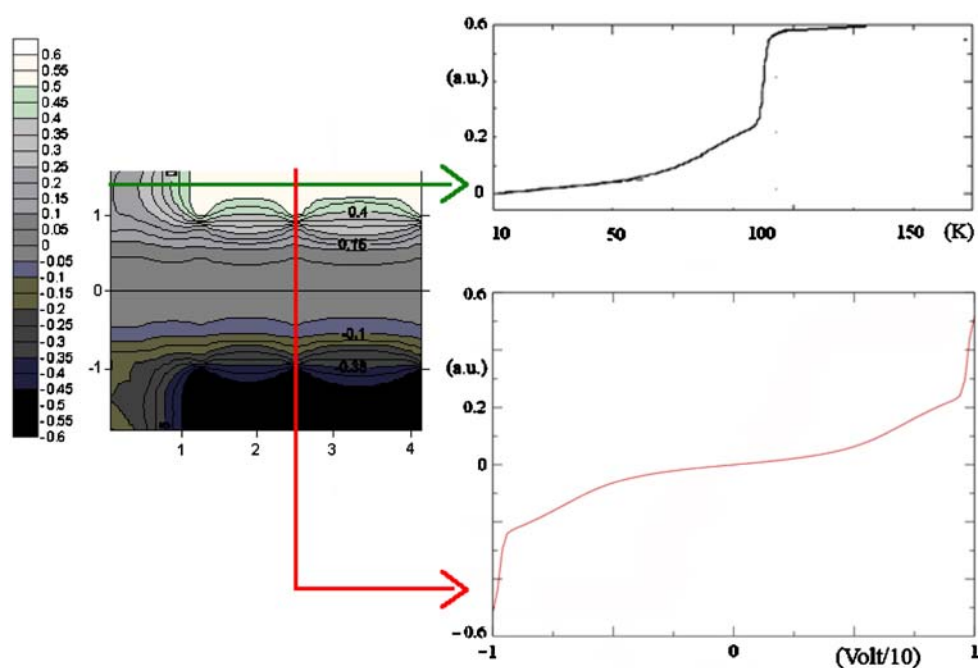
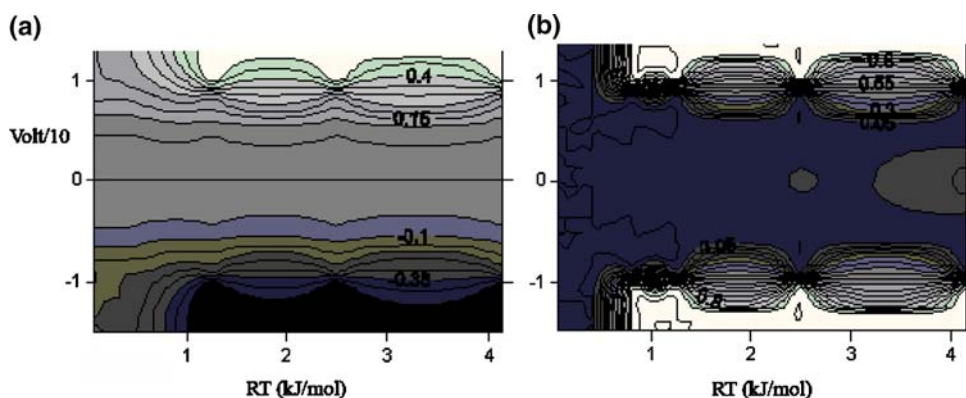


Fig. 4 Inset a ICT, $\langle \Delta q \rangle_n$ (a.u.) reported on the plane of temperature (reported in abscissa as RT , kJ/mol) and applied voltage (in volt/10) for OPE1. Inset b Cumulative probability of non-planar OPE1 conformations (1b and 1g) reported on the plane of temperature (reported in abscissa as RT , kJ/mol) and applied voltage (in volt/10) for OPE1



(formal) chemical equilibrium



It means that during experimental measurements, at the stationary conditions, the actual species responsible of the conductance could be reduced OPEs.

In order to investigate the role of the reduced species in ICT process, we used the following coherent, although ideal, model reported in the Scheme 1.

Let us consider gaseous OPE molecule and gold surface of the electrode at lower potential (the electronic donor) as never mutually interacting.

In the first step, one electron is extracted from the gold electrode at fixed electric potential $V = V_{\text{Au}}$, i.e. the free electron is at the same electric potential of the electrode.

In the second step, the electric potential of the free electron is changed to match the OPE potential V_{OPE} , i.e. the electric

potential at the OPE and OPE^- geometrical centre which has been used in PMM calculations to obtain the perturbed electronic states. In the final step, the gaseous OPE is reduced with a free energy variation given by Eq. (11). The maximum work related to the above process may be therefore evaluated by the equation:

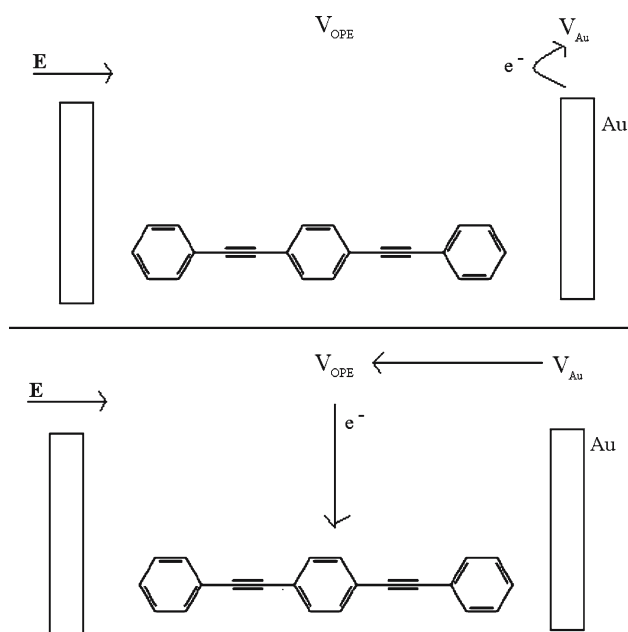
$$\Delta A_{\text{overall}}(E) = \text{WF} + \Delta A(E) + e(V_{\text{OPE}} - V_{\text{Au}}) \quad (14)$$

where e is the electronic charge and WF is the gold work function in vacuum (5.3 eV) [19].

Note that in the last equation we neglect the electric field effect on gold WF (i.e. on the gold fermi level) [29].

The free energy curves for both OPE molecules, as provided by Eq. (14), are given in Fig. 5.

Not surprisingly, in the absence of applied field, gaseous OPEs are hardly reducible at 300 K. However, it exists a voltage for which anionic forms become well accessible



Scheme 1 Ideal scheme for the calculation of OPE reduction thermodynamics

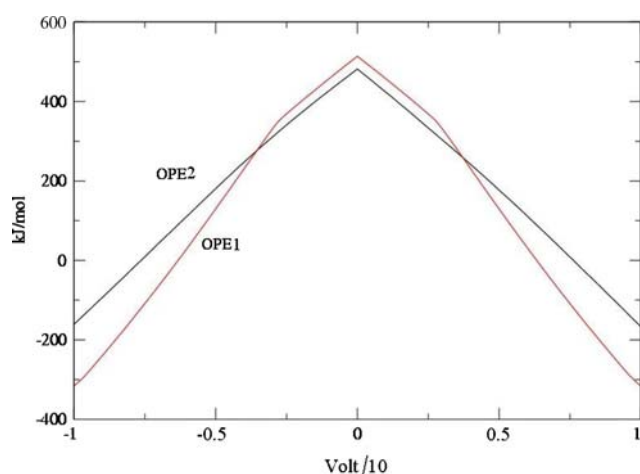


Fig. 5 Maximum work related given by Eq. (14) at 300 K, for the reduction of OPE1 (red curve) and OPE2 (black curve) as a function of the applied voltage along OPE (see text)

($\Delta A_{\text{overall}} = 0$). Our idealised model indicates such chemical transitions to occur at formal voltages of ± 5.1 V and ± 6.7 V for OPE1 and OPE2, respectively.

Using the free energy curves of Fig. 5 we may evaluate the actual ICT expectation value, weighted by the relative probability of neutral and reduced OPE.

For this purpose we calculated the molecular fraction of reduced OPE (X_r) using the standard relation

$$X_r = \frac{\exp(-\beta \Delta A_{\text{overall}}(\mathbf{E}))}{1 + \exp(-\beta \Delta A_{\text{overall}}(\mathbf{E}))} \quad (15)$$

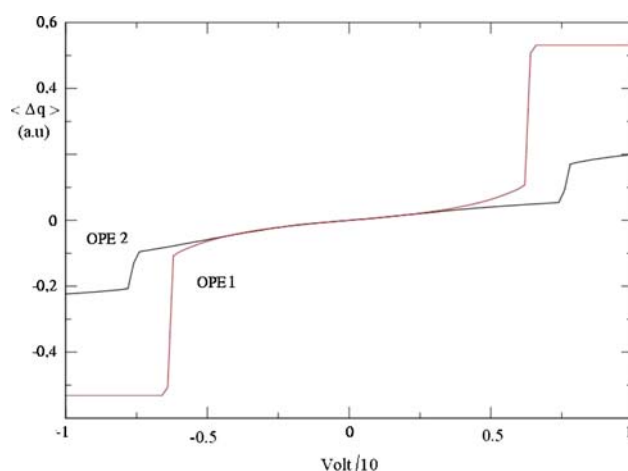


Fig. 6 Overall ICT (calculated using Eq. (16)) for OPE1 (red) and OPE2 (black) as a function of the applied voltage along OPE (see text)

and, consequently, the actual observed ICT in the presence of an applied electric field

$$\langle \Delta q \rangle = X_r \langle \Delta q \rangle_r + (1 - X_r) \langle \Delta q \rangle_n \quad (16)$$

The Application of Eqs. (15) and (16) provides the overall charge separation at 300 K, shown in Fig. 6, now including the chemical redox equilibrium. From Fig. 6 it follows that both OPE molecules present highly non-linear ICT as a result of the reduction process (see for comparison Fig. 3).

However, even considering the redox process, the ICT switch for OPE1 is considerably larger than in OPE2. Interestingly both systems, approaching 10 V, reach a plateau probably indicating a saturation.

Finally it is worth noting that, although for the neutral OPE1 conformational equilibria play a major role in modulating ICT (see Fig. 4), for the reduced form given the high intrinsic conductivity of the molecule, all the accessible conformations provides similar ICT behaviour.

4 Conclusions

In this work we have investigated, by using MD simulations and PMM calculations, the effect of the temperature and oxidation state variations on the electronic properties of OPE molecules in the presence of an external homogeneous electric field. Results indicate that non-linear Intramolecular Charge Transfer, induced by a proper electric field, is related to OPE conformational transitions but also to OPE chemical alterations, i.e. electron transfer reactions. This produces a potentially strong effect of the temperature on OPE1 and OPE2 electric properties. The present investigation, whose aim was not to model molecular conduction for which other specialized methodologies are present in the literature, clearly indicates the necessity of including thermal and chemical

effects for a more realistic description of molecular conductance at atomic-molecular level, at least when flexible molecules like OPEs are concerned.

Acknowledgments We wish to acknowledge CASPUR (Roma) for the use of Gaussian03. We also wish to thank an unknown referee for important suggestions improving the quality of the present work.

References

1. Moore GE (1965) *Electronics* 38:114
2. Aviram A, Ratner MA (1974) *Chem Phys Lett* 29:277
3. Janata J (2003) *Phys Chem Chem Phys* 23:5155
4. Haiss W, Nichols RJ, van Zalinge H, Higgins SJ, Bethell D, Schiffrin DJ (2004) *Phys Chem Chem Phys* 27:4330
5. Nitzan A, Ratner MA (2003) *Science* 300:1384
6. Troisi A, Ratner MA (2007) *Phys Chem Chem Phys* 19:2421
7. Yaliraki SN, Roitberg AE, Gonzalez C, Mujica V, Ratner MA (1999) *J Phys Chem* 111:6997
8. Derosa PA, Seminario JM (2001) *J Phys Chem B* 105:471
9. Brandbyge M, Mozos JL, Ordejon P, Taylor J, Stokbro K (2002) *Phys Rev B* 65:165401
10. Taylor J, Guo H, Wang J (2001) *Phys Rev B* 63:121104R
11. Li Y, Zhao J, Yin X, Liu H, Yin G (2007) *Phys Chem Chem Phys* 9:1186
12. Schnurpfeil A, Albrecht M (2007) *Theor Chem Acc* 117:29–39
13. Haiss W, van Zalinge H, Bethell D, Ulstrup J, Schiffrin DJ, Nichols RJ (2006) *Faraday Discuss* 131:253
14. See Jones DR, Troisi A (2007) *J Phys Chem C* 111:14567 and references therein
15. Amadei A, D'Abramo M, Di Nola A, Arcadi A, Cerichelli G, Aschi M (2007) *Chem Phys Lett* 434:194
16. Aschi M, Di Nola A, Spezia R, Amadei A (2001) *Chem Phys Lett* 344:374
17. Seminario JM, Zacarias AG, Derosa PA (2001) *J Phys Chem A* 105:791 and references therein
18. Taylor J, Brandbyge M, Stokbro K *Phys Rev B* 68(303):121101(R)
19. He J, Fu Q, Lindsay S, Cizek JW, Tour JM (2006) *J Am Chem Soc* 128:14828 and references therein
20. McCreery RL, Wu J, Kalakodimi RP (2006) *Phys Chem Chem Phys* 22:2572
21. Evans DJ, Morriss GP (1990) *Statistical mechanics of nonequilibrium liquids*. Academic Press, London
22. Amadei A, Chillemi G, Ceruso MA, Grottesi A, Di Nola A (2000) *J Chem Phys* 112:9
23. Hess B, Bekker H, Berendsen HJC, Fraaije JGEM (1997) *J Comput Chem* 18:1463
24. van der Spoel D et al (1996) *Gromacs user manual* 1.3
25. Amadei A, Linssen ABM, Berendsen HJC (1993) *Proteins Struct Funct Gen* 17:412
26. Perdew JP, Burke K, Ernzerhof M (1996) *Phys Rev Lett* 77:3865
27. Gaussian 03 (2004) Gaussian Inc., Wallingford
28. Greaves SJ, Flynn EL, Fletcher EL, Wrede E, Lydon DP, Low PJ, Rutter SR, Beeby A (2006) *J Phys Chem. A* 110:2114
29. Han W, Durantini EN, Moore TA, Gust D, Rez P, Leatherman G, Seely GR, Tao N, Lindsay SM (1997) *J Phys Chem* 101:10719